Detonation Propulsion for High Pressure Environments

LLOYD H. BACK* AND GIULIO VARSI†
Jet Propulsion Laboratory, Pasadena, Calif.

One limitation encountered by chemical rocket propulsion in high-pressure planetary atmospheres is illustrated by the conflict between the dependence of specific impulse on the ratio of chamber pressure to ambient pressure and the dependence of the motor structural design on the difference between the pressures. This work proposes to resolve the difficulty by employing detonating propellant in which the high pressures necessary for efficient propulsion are developed over a short time and need not be contained statically. Experimental results are presented to substantiate this claim of relatively high performance, together with an analytical development that approximately describes the flow dynamics.

Nomenclature

A = nozzle cross-sectional area
c_a = speed of sound in ambient gas
C_D = flow coefficient
e_α = specific energy released in explosion, E_α/m_e
E_α = energy released in explosion
E_α' = energy released per solid angle, E_α/ω
$f_1 f_2$ = functions of γ, Eq. (15)
f_3 = function, Eq. (19)
F = axial thrust
g = acceleration of gravity
g_c = conversion constant
G = integral, Eq. (16)
H = integral, Eq. (16)
H_t = total enthalpy
Δh = height
I = specific impulse
L = axial length of nozzle
m = mass of gas
m_a = mass of ambient gas contained in nozzle
m_e = mass of explosive material
$\dot{m}$ = mass flow rate
M = mass of equipment
M_w = molecular weight
P = static pressure
P_a = ambient pressure
P_o = plateau pressure
Δp = pressure difference, $P_t - P_a$
r = radial distance from apex of cone
r_e = effective radial length of nozzle, Table 4
R = gas constant
R_u = universal gas constant
R_l = characteristic radial length, Eq. (17)
t = time
T = temperature
u = velocity
V = volume
z = elevation
α = function of γ, Table 3
γ = specific heat ratio
ε = expansion area ratio of nozzle
θ = divergent half-angle of nozzle
λ = divergence factor
ρ = density
σ = ratio of mass of ambient gas in nozzle to mass of gas generated from explosion, m_a/m_e
τ_e = nondimensional time until shock wave reaches nozzle exit, $t_e c_a/R_l$
ω = solid angle

Subscripts

a = ambient condition
e = condition at nozzle exit
t = stagnation condition
th = nozzle throat

Presented as Paper 73-1237 at the AIAA/SAE 9th Propulsion Conference, Las Vegas, Nev., November 5–7, 1973; submitted November 29, 1973; revision received March 11, 1974. The authors acknowledge the imaginative leadership of W. Dowler and A. Murphy in this effort and thank D. Davis for the skillful design of the experiments and S. Gill of Artec Associates, Hayward, Calif., for some suggestions on the use of a nozzle in a detonating system. This work presents the results of one phase of research carried out in the Propulsion Division of the Jet Propulsion Laboratory, California Institute of Technology, under Contract NAS7-100, sponsored by NASA.

Index categories: Shock Waves and Detonations; Combustion Stability, Ignition, and Detonation; Electric and Advanced Space Propulsion.

* Member Technical Staff. Associate Fellow AIAA.
† Senior Scientist. Member AIAA.

I. Introduction

THE presence of dense atmospheres on several planets, terrestrial as well as extraterrestrial, poses a new challenge to the design of spacecraft. The difficulty specifically encountered in the design of the propulsion system is illustrated in Fig. 1. Here the specific impulse obtained from anhydrous hydrazine (80% ammonia dissociated molecular weight of 11.7 g/g-mole and $\gamma = 1.32$) is computed as a function of ambient pressure P_a for a combustion temperature of 1000°K, nozzle flow coefficient

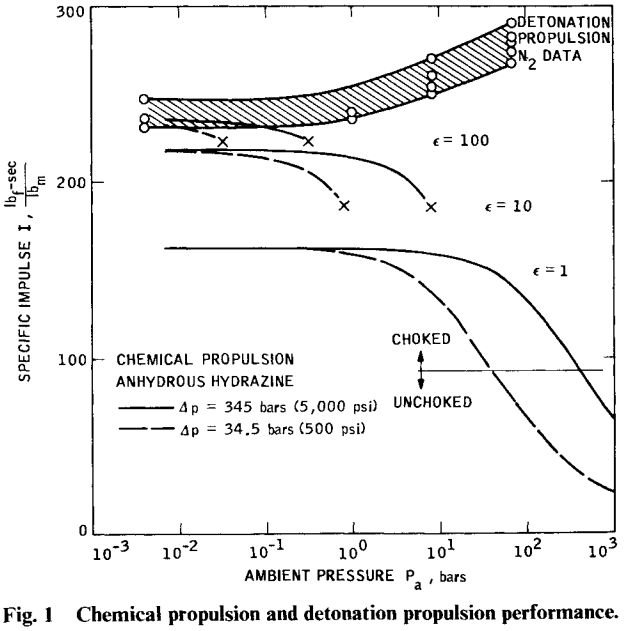

Fig. 1 Chemical propulsion and detonation propulsion performance.

Table 1 Planetary ambient pressures

Z, km	Pressure range (bars) Venus[a]	Jupiter[b]	Saturn[c]
50	1	0.08	0.3
0	95	1	1
−170	—	30	10
−280	—	100	25

[a] Ref. 11.
[b] Ref. 15.
[c] Ref. 16.

C_D of 0.95, and a divergence factor λ of unity for nozzles with various expansion area ratios ε. The relationships used in these calculations are given in the Appendix. The combustion and stagnation pressure is not kept constant but instead is increased as the ambient pressure increases so that the pressure difference Δp across the chamber wall remains constant. This constraint is imposed to limit the maximum stress that the materials used must withstand at a given chamber temperature. The performance curves indicate the penalty imposed for operation at higher ambient pressures where nozzles with smaller expansion area ratios would be required to extend the operating range. The crosses denote the maximum ambient pressure before shock-induced flow separation would occur in the nozzle, and thus limit the utilization of larger expansion area ratio nozzles which have a better performance. For perspective, the ranges of ambient pressures of interest in the exploration of planets are shown in Table 1.

The question may be asked at this point, why attempt to use rockets at all since on Earth, aerodynamic surfaces and air breathing engines have provided a very successful solution to the requirement of mobility in the atmosphere?

In fact, if only a landing operation is required, aerodynamic surfaces and deployable parachutes appear as a very adequate solution. There are, however, several reasons why active propulsion and attitude control will be necessary: a) accurate imaging capability; b) sample return; c) information transmission (when the absorption coefficient of the atmosphere forbids radio transmissions, a probe that can periodically "surface" and transmit the data gathered in depth can offer an advantageous alternative to a series of stacked "repeater" probes); and d) severe atmospheric turbulence (such as 100 msec^{-1} Jupiter winds).

In such cases, the aerodynamic surfaces will have to be designed to withstand and operate in: a) widely varying density and pressure regimes (5 orders of magnitude); b) unknown conditions of flow dynamics; and c) very severe entry conditions (ablation loss of the order of 35% is required for Jupiter entry).

No aerodynamic structure has ever been designed for such conditions and even in the Earth atmosphere, airfoils that are deployable in motion have been extremely difficult to build.

There is therefore a need for considering rocket propulsion for the dense atmospheres of the planets, if somehow the chamber pressure could be increased. The idea that can be pursued is that if the operation of the rocket is intermittent, the impulse being delivered in many short bursts, the "chamber" pressures would not have to be contained statically (such as in conventional rockets) but only dynamically for a few microseconds where the inertia forces of the materials and not only their tenacity could be exploited.

It becomes then a very natural step to explore the use of a detonating propellant which develops detonation pressures of 20–200 kbar in comparison to which any atmospheric pressure of interest (up to a few kilobars) becomes negligible. Such a system would be insensitive to pressure in the sense that its expansion ratio would be practically infinite and able to function equally well in a vacuum and in the dense atmosphere. This circumstance is very fortunate because it would eliminate the need for a vacuum propulsion system and a separate atmospheric propulsion system.

Early conceptual designs evolving from flier plate techniques employed alternating layers of solid high-explosive wafers and attenuating low-density materials in an attempt to reduce the peak shock strength and to spread the resultant pressure pulse over a longer period of time.[1] The stacked array of explosive charges and attenuators was attached to the payload through a shock-absorbing device patterned after a configuration developed for the Orion Project simulation experiments. Various design options were proposed in which the discrete explosive layers could be initiated sequentially but independently upon command, or by shock waves generated by the detonation of preceding charges as in a conventional explosive train. Because these designs were formulated without the use of a combustion chamber or nozzle, a significant reduction in the inert mass was postulated. Very large increases in specific impulse over conventional solid-propellant rockets were claimed for near-Earth applications.[1]

Clearly the energy released per unit mass by a chemical explosive is of the same order (5–7 Mjoules · kg^{-1}) as available in chemical propellants. In addition, the maximum specific impulse achievable by explosives is somewhat less than that derived from conventional propellants because the conversion of thermal energy into momentum of resultant gases is less efficient in a detonation than in a nozzle expansion. Further, the nonuniformity of the velocity distribution of detonation gases causes a loss in specific impulse, which has been calculated to be of the order of 15%.[2]

Numerical analyses by one-dimensional hydrodynamic codes have shown that the specific impulse theoretically obtainable by a conventional explosive, detonating against a steel acceptor plate, is approximately 2160–2450 N · sec · kg^{-1} (220–250 lb$_f$ · sec · lb$_m^{-1}$).[2,3] The effect of a 15° nozzle of infinite length has also been calculated with a one-dimensional hydrodynamic code[2] and an increase in specific impulse of about 20% was predicted.

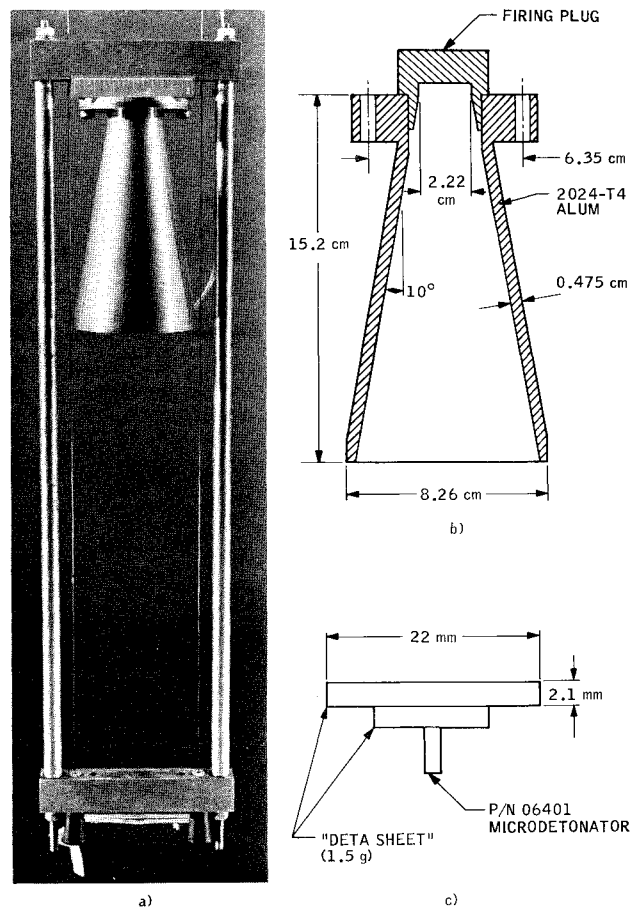

Fig. 2 Experimental device.

Table 2 Experimental data

Run No.	Nozzle half-angle (degrees)	Nozzle length (cm)	Ambient gas Type	Pressure (bars)	Temperature °C	Density gm/cm³	Specific impulse I (sec)[d]	σ m_a/m_e
1.16[a]	—	0	N_2	4×10^{-3}	25°	4.52×10^{-6}	154	—
1.17[a]	↓	↓	N_2	1	25°	1.13×10^{-3}	169	—
1.18[a]	↓	↓	N_2	8.28	25°	9.36×10^{-3}	159	—
1.19[a]	↓	↓	N_2	69	25°	77.97×10^{-3}	143	—
1.12	10°	3.8	N_2	8×10^{-3}	25°	9.04×10^{-6}	222	1.5×10^{-4}
1.13	↓	↓	N_2	1	25°	1.13×10^{-3}	237	1.90×10^{-2}
1.14	↓	↓	N_2	8.28	25°	9.36×10^{-3}	260	1.57×10^{-1}
1.15	↓	↓	N_2	69	25°	77.97×10^{-3}	282	1.31
1.8	10°	7.6	N_2	4×10^{-3}	25°	4.52×10^{-6}	232	2.4×10^{-4}
1.9	↓	↓	N_2	1	25°	1.13×10^{-3}	239	5.90×10^{-2}
1.10	↓	↓	N_2	8.28	25°	9.36×10^{-3}	254	4.90×10^{-1}
1.11	↓	↓	N_2	69	25°	77.97×10^{-3}	267	4.1
1.4	10°	11.4	N_2	4×10^{-3}	25°	4.52×10^{-6}	249	5.1×10^{-4}
1.5	↓	↓	N_2	1	25°	1.13×10^{-3}	236	1.28×10^{-1}
1.6	↓	↓	N_2	8.28	25°	9.36×10^{-3}	250	1.06
1.7	↓	↓	N_2	69	25°	77.97×10^{-3}	279	8.87
1.1	10°	15.2	N_2	4×10^{-3}	25°	4.52×10^{-6}	236	9.4×10^{-4}
140 C1	↓	↓	Air	1	25°	1.17×10^{-3}	219–236	2.44×10^{-1}
1.2	↓	↓	N_2	8.28	25°	9.36×10^{-3}	270	1.95
1.3	↓	↓	N_2	69	25°	77.97×10^{-3}	290	16.2
2.3[b]	0°	21.0	N_2	6.7×10^{-3}	25°	7.57×10^{-6}	231	4.0×10^{-4}
2.1[b]	↓	↓	N_2	1	25°	1.13×10^{-3}	214	6.00×10^{-2}
2.2[b]	↓	↓	N_2	69	25°	77.97×10^{-3}	273	4.14
3.1	70°	1.5	N_2	10.7×10^{-3}	25°	12.09×10^{-6}	203	4.2×10^{-4}
3.2	↓	↓	N_2	1	25°	1.13×10^{-3}	211	3.94×10^{-2}
3.3	↓	↓	N_2	69	25°	77.97×10^{-3}	143	2.72
C1.5	10°	15.2	CO_2	1	35°	1.75×10^{-3}	255	0.37
C1.4	↓	↓	CO_2	25.3	35°	4.55×10^{-2}	307	9.5
C1.3	↓	↓	CO_2	47.3	35°	9.95×10^{-2}	338	20.8
C1.2	↓	↓	CO_2	69.7	35°	2.02×10^{-1}	378	41.2
C1.1	↓	↓	CO_2	84.5	35°	5.73×10^{-1}	579	120
—[c]	10°	3.8	Sand	1	25°	1.75	560	29.4
310[c]	10°	15.2	Microballoons	1	25°	1.6×10^{-1}	615	33.5
320[c]	↓	↓	Microballoons and water	1	25°	5.67×10^{-1}	1158	119
330[c]	↓	↓	Water	1	25°	1	2115	209

[a] No nozzle, only a flat plate of the same diameter as the firing cup 2.22 cm (= 7″/8).
[b] A cylindrical tube with internal diameter = 2.22 cm (= 7″/8).
[c] These experiments were performed in air; the nozzle was filled with the materials indicated.
[d] Units of specific impulse are lb_f-sec/lb_m. For conversion to the SI system (N-sec/kg), the tabulated values are to be multiplied by the factor 9.806.

Only recently, significant developments[4–6] in this propulsion concept that utilizes propellant detonating at the throat of a supersonic expanding nozzle have occurred both experimentally and theoretically.

The current analytical effort at the Jet Propulsion Laboratory consists first of an adaptation of blast wave theory which approximates the process by neglecting the mass of the propellant in comparison with the mass of ambient gas present in the nozzle and applying to this gas the energy released by the explosion. Secondly, monodimensional numerical calculations are being performed with standard hydrodynamic computer codes which can describe the interaction between the products of explosion and the ambient gas. More complete two-dimensional numerical calculations are planned.

The relative independence of performance, measured by the specific impulse, on ambient pressure, is borne out by the analysis outlined above and by experimental data as discussed later. Furthermore, both analysis and experiments show a favorable dependence of performance on density of the ambient gases. This effect is fundamentally understood in terms of expelling from the nozzle a mass of gas which is greater, the greater the density; since this mass is not carried on the spacecraft and therefore is not counted as propellant, its effect is beneficial and generates an increase of performance approximately proportional to the square root of the density of ambient gas.

II. Experiments

The experiments were directed toward a determination of the specific impulse with different ambient gases and pressures; changes in the nozzle geometry were also explored. The device used consisted of the aluminum structure, shown in Fig. 2a. Friction against the guy wires was minimized by operating with vertical motion and by using Teflon bushings. Several nozzles were employed: the most often used, 15 cm long, is shown in Figs. 2a and 2b.

A simple shock absorber consisting of a stack of masonite, aluminum, and steel, respectively, 3.2, 3.2, and 6.4 mm thick, was inserted between the upper beam of the sled and the firing cup.

The impulse was determined by measuring the maximum height Δh reached by the sled as a result of firing of the explosive according to:

$$\int F dt = M(2g\Delta h)^{1/2} \tag{1}$$

where g is the acceleration of gravity and M is the mass of the equipment. The height Δh was measured by means of a marker (a steel spring) raised by the sled during its upward motion and left in position, because of friction against the guy wire, during the descent of the sled.

The high-pressure environment was provided by placing the assembly consisting of sled, guy wires, and supports in a cylindrical tank (diam = 40 cm, length = 70 cm) which prior to firing was filled with the desired gas and pressurized as required up to a maximum of 85 bars. The travel of the sled was limited to about 5–10 cm by adding a payload of lead spheres to the top of the sled itself so that M was over a thousand times larger than the mass of the explosive propellant. The marker permitted a maximum reading accuracy of 1.5 mm corresponding to an estimated error of 1–2% in the computed impulse.

Attention was placed on the elimination of a secondary impulse following that generated by the detonation wave in the nozzle, when the shock reflected by the tank bottom impinged on the nozzle. This effect was attenuated below the sensitivity of the measurements by arranging a random packing of No. 00 steel wool approximately 25 cm thick on the bottom of the tank.

The explosive propellant used throughout the ballistic tests was a commercial product, "deta-sheet A" manufactured by DuPont de Nemours, Wilmington, Del., and nominally composed of 85% PETN (Pentaerythritol tetranitrate) and 15% binding wax. The mass of the propellant used on all experiments was 1.5 g configured as shown in Fig. 2c; the explosive thickness was doubled as shown to obtain reliable and complete detonation. The Space Ordnance Systems, Inc., P/N 06401 microdetonator containing 0.032 g of explosive was held in place by adhesive tape. The explosive energy released per mass of explosive was $e_\alpha = 1180$ cal/g.

The measurements were made at an ambient temperature of 25°C except for carbon dioxide for which the temperature was 35°C. Strip heaters to preheat carbon dioxide to the vicinity of its critical temperature ($T_c = 31$°C) were located around the outside of the tank in which these tests were made. The higher test pressures were in the vicinity of the critical pressure ($P_c = 74$ bars) for carbon dioxide and the ambient densities were obtained from the measurements of Michels, et al.[7,8]

The reported values of the specific impulse I were obtained by dividing the impulse by the mass of the explosive:

$$I = \int F dt / g_c m_e = M(2g\Delta h)^{1/2}/g_c(1.532 \times 10^{-3}\,\text{kg}) \tag{2}$$

The experimental results are reported in Table 2 and some of the data are also shown in Fig. 1 to indicate the higher performance achieved relative to a chemical propulsion system. The results are discussed subsequently in the following sections.

Further Developments

To obtain a rocket motor suitable for space flight it is necessary to design a configuration in which several firings can be accomplished with a minimum of auxiliary mass such as detonators and wiring, and with a degree of flexibility as to repetition rate and size of charges.

It is appropriate to explore the use of a fluid explosive, not necessarily liquid, which can be detonated remotely. Several schemes have been advanced for firing, including: hypergolic mixtures, radiofrequency waves, and microwaves[9] to deliver energy to submillimeter receiving elements imbedded in the propellant, and focused laser beams. Two formulations have been prepared[10] that can be handled safely and can be initiated with a 20 joule laser beam focused by a 30 cm focal distance lens. These formulations are suspensions of ground crystalline explosive in Bis(2, 2-dinitro-2-fluoro-ethyl) formal (FEFO).

III. Experimental Data and Trends

The variation of specific impulse obtained with nitrogen and carbon dioxide as the ambient gases is shown in Fig. 3 as a function of the ratio of the mass of ambient gas m_a contained in the nozzle to the mass of gas generated from the explosive material (m_e for an ideal explosion):

$$\sigma = m_a/m_e \tag{3}$$

This is an important parameter in detonation propulsion, as will be seen subsequently. The general trend exhibited by the data

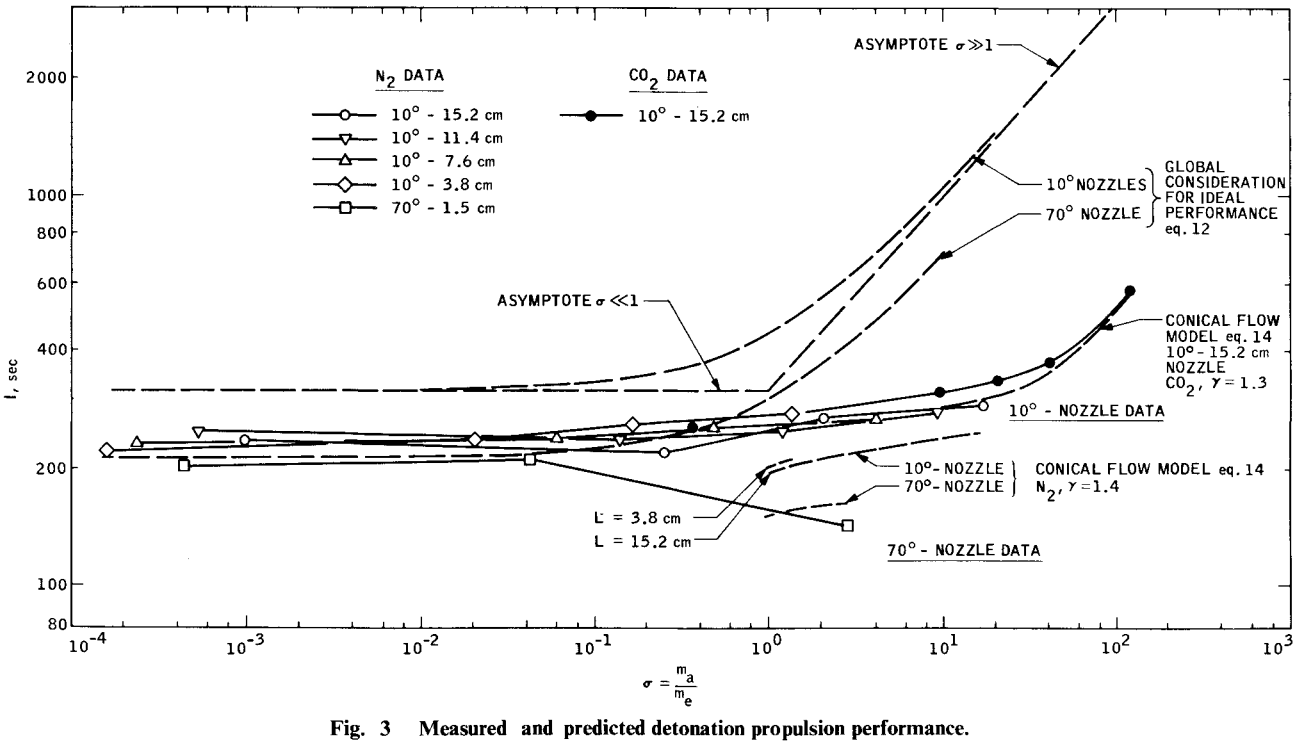

Fig. 3 Measured and predicted detonation propulsion performance.

indicates that the specific impulse is relatively constant (approximately 230 sec) at relatively small values of σ and then begins to increase for values of σ of order 0.1. The increase in specific impulse is greater for larger values of σ with a value of about 580 sec achieved with carbon dioxide.

The larger angle nozzle does not follow the trend observed for the smaller angle nozzles as σ increases presumably because the momentum interaction between the explosive and ambient gases is nonuniform across the nozzle with such a relatively large divergent half angle of 70°. Smaller half-angle nozzles apparently confine the momentum interaction laterally and the performance increases with σ.

The specific impulse obtained with other materials is indicated in Table 2. A value as large as 2100 sec was achieved with the nozzle filled with water. "Microballoons" denotes epoxy spheres of diameter ranging from 1.3 mm–3.2 mm: these were used dry and with water to obtain various densities for the medium in the nozzle.

IV. Global Considerations

The experimental trends are discussed in this section in terms of global considerations to establish a reference datum to appraise the impulsive performance.

When σ is relatively small compared to unity the specific impulse is essentially associated with the momentum, $m_e\bar{u}$, of the explosive gas exhausted from the nozzle, and therefore the effect of ambient density or pressure should have little influence on the performance. For the nitrogen and/or air measurements the mass of ambient gas in a nozzle of volume V is directly related to ambient pressure P_a and temperature T_a through the perfect gas relation:

$$m_a = M_w P_a V / R_u T_a$$

where M_w is the molecular weight of the ambient gas and R_u is the universal gas constant. For nonideal gas behavior, the corresponding relation is

$$m_a = \rho_a V$$

However, when σ becomes of order 0.1 and larger, the shock wave that is produced by the hot exploded matter initially at very high pressures becomes important. This shock wave propagates along the nozzle and engulfs the denser ambient gas contained in the nozzle, setting it into motion. In this manner, the ambient gas contributes to the specific impulse too because of its momentum $m_a\bar{u}$. This salient feature makes detonation propulsion attractive in regions where the ambient density and thus mass of ambient gas is relatively large, such as in the planetary atmosphere of Venus.

To place these ideas on a quantitative basis but still without the details of the actual flow and wave phenomena involved, a simplified analysis based on first principles is considered. This involves the application of the axial momentum balance to a mass of gas m in the nozzle that is presumed to be accelerated to an average velocity $\bar{u}$ and is exhausted from the nozzle at the ambient pressure

$$\int F dt = m\bar{u}_z = \lambda m\bar{u} \tag{4}$$

In this relation, λ is the divergence factor

$$\lambda = \tfrac{1}{2}(1+\cos\theta) \tag{5}$$

applicable for a conical nozzle with divergent half-angle θ. For small angles θ, $\lambda \to 1$, and as $\theta \to 90°$, $\lambda \to \frac{1}{2}$.

If all of the energy released in the explosion E_α goes into increasing the total enthalpy H_t of the mass of gas m, and this thermal energy in turn is converted completely into kinetic energy ($\bar{u}^2/2$), then since

$$E_\alpha = mH_t \quad \text{and} \quad \bar{u} = (2g_c H_t)^{1/2} \tag{6}$$

the specific impulse obtained from its definition, Eq. (2) and Eqs. (4) and (6), is given by

$$I = \lambda(2me_\alpha/g_c m_e)^{1/2} \tag{7}$$

where e_α is the energy released in the explosion per mass of explosive, i.e., E_α/m_e. In Eq. (6) the initial enthalpy of the mass of gas was neglected since it is generally negligible compared to the relatively large amount of explosive energy released.

When the parameter σ is small, i.e., $\sigma \ll 1$, the effective mass of gas in the nozzle is that of the explosive gas, i.e., $m \simeq m_e$. From Eq. (7), the specific impulse is independent of the ambient pressure or density and is given by

$$I = \lambda(2e_\alpha/g_c)^{1/2} \tag{8}$$

In particular for a typical high explosive such as detasheet, the calculated value is

$$I = \lambda(320)\,\text{sec}$$

The measured value of I for the smaller half-angle nozzles is about $\frac{3}{4}$ of this maximum value (Fig. 3), presumably because not all of the thermal energy is converted into kinetic energy as implied ideally in Eq. (6), and therefore the momentum of the explosive gas, $\lambda m_e\bar{u}$, is overestimated. The influence of the divergence factor λ appears to be in the same direction as indicated by the data (Fig. 3), although relative differences are also associated with nonuniform flow effects believed to be present in the large divergent half-angle nozzle.

The more important situation is when the parameter σ is relatively large, i.e., $\sigma \gg 1$, and the effective mass of gas in the nozzle is essentially the ambient gas, i.e., $m \simeq m_a$. Then Eq. (7) becomes

$$I = \lambda(2m_a e_\alpha/g_c m_e)^{1/2} \tag{9}$$

For a given nozzle of volume V, the basic dependence of the mean specific impulse on ambient conditions is given by the following relation if the ambient gas behaves in an ideal way:

$$I \propto (M_w P_a/T_a)^{1/2} \tag{10}$$

For nonideal gas behavior, the more general relation is

$$I \propto (\rho_a)^{1/2} \tag{11}$$

These relations indicate the enhanced performance anticipated at higher ambient densities. The asymptotic value for $\sigma \gg 1$ is shown in Fig. 3 along with the general relation for any σ given by Eq. (7); i.e., with $m = m_a + m_e$

$$I = \lambda(2e_\alpha/g_c)^{1/2}(1+\sigma)^{1/2} \tag{12}$$

Although the experimental specific impulse does increase with σ, the square root dependence on σ is larger than observed until values of σ are on the order of 100, as indicated by the carbon dioxide data. The global values also are considerably larger than observed. The momentum of the ambient gas, $\lambda m_a\bar{u}$, is overestimated by virtue of Eq. (9) as was also the case for the other limiting regime $\sigma \ll 1$, but probably more for the case of $\sigma \gg 1$ because of the reduced strength of the shock wave that propagates along the nozzle setting the ambient gas into motion with relatively lower speeds. Clearly, in order to obtain more definitive information, analysis of the actual flow and wave phenomena is required.

V. Flow and Wave Motion—Conical Flow Theory

Blast wave theory was applied in Ref. 5 to determine the impulsive performance of detonating an explosive in a conical nozzle for the situation where $\sigma \gg 1$; i.e., for the case where the mass of ambient gas in the nozzle is relatively large compared to the mass of gas m_e produced by the explosion, a contention of particular interest for relatively dense atmospheres. In the model, instantaneous detonation and energy release was presumed to occur at a point located on the apex of a conical nozzle with half angle θ. The shock wave generated by the explosion was taken to propagate as a spherical wave along the nozzle, thereby setting the ambient gas into one-dimensional radially outward motion. In this simplified view, the detailed nature of the initiation and kinetics of the explosion and the formation of the shock wave along with other wave motion were not considered; nor were the actual configurations of the charge, nozzle throat, and endwall accounted for. Frictional effects along the wall, heat transfer to the wall, and any dissociative effects of shock heating were also neglected. The ambient gas contained in the nozzle was taken to be a perfect gas with a constant value of γ so that

existing solutions from blast wave theory could be utilized. General relations were given for an arbitrary value of γ, and in particular, specific results were presented for an ideal diatomic gas or a mixture of diatomic gases such as air with $\gamma = 1.4$.

The axial thrust and thus impulse was obtained by integrating the pressure distribution along the conical wall, taking the axial component and then integrating over the duration of the expulsion, rarefaction and refilling phases

$$\int F dt = 2\pi \sin^2\theta \int_o^\infty \int_o^R (P - P_a) r dr\, dt \tag{13}$$

For the conditions of the experiments it was possible to carry out the integration in two parts, the first part until the time t_e when the shock wave reached the nozzle exit and the second part for the remainder of the contribution for $t > t_e$, i.e., when the shock wave has passed outside the nozzle, by simplifying some of the integrals to obtain the following approximate closed form analytical relation for the specific impulse including counterpressure effects

$$I = \left[\frac{16}{15}(2)^{1/2}\pi\right]\left[\frac{\sin^2\theta r_e^{3/2}}{(1-\cos\theta)^{1/2}}\right] f_1 \frac{e_\alpha^{1/2}\rho_a^{1/2}}{m_e^{1/2} g_c^{1/2}} \times \left[1 + \frac{15}{32(\pi)^{1/2}} f_2 H \left(\frac{r_e}{R_l}\right)^{1/2}\right] \tag{14}$$

where the functions f_1 and f_2 depend on γ

$$f_1 = G(\gamma+1)^{-1}\alpha^{-1/2}; \quad f_2 = (\gamma+1)\alpha^{1/2}\gamma^{-1/2}G^{-1} \tag{15}$$

and the integrals G and H are given by

$$G = \int_o^1 \frac{p}{p_R}\frac{r}{R} d\left(\frac{r}{R}\right); \quad H = \int_{\tau_e}^\infty \left(\frac{P_o}{P_a} - 1\right) d\tau \tag{16}$$

Various quantities that appear in these expressions are identified in the nomenclature.

This particular form indicating the explicit dependence upon the quantities of interest can be used for values of the ratio of the radial nozzle length r_e to characteristic length R_l; i.e., r_e/R_l to about unity without too much error. The expression for the characteristic length R_l is given by

$$R_l = (E_\alpha'/P_a)^{1/3} = e_\alpha^{1/3}(m_e/\omega P_a)^{1/3} \tag{17}$$

where ω is the solid angle, $2\pi(1 - \cos\theta)$. The length R_l which is important in detonation propulsion corresponds to the location where the shock Mach number has decayed to a value of a little less than 2 and is the approximate location where the plateau pressure P_o behind the shock wave drops below the ambient pressure signifying the onset of the rarefaction phase (see Ref. 5, Fig. 3).

Dependence on γ

The calculations presented in Ref. 5 for $\gamma = 1.4$ are extended herein to an ideal triatomic gas $\gamma = 9/7 = 1.29 \simeq 1.3$ so that the analysis can be applied to other gases such as carbon dioxide, the primary component in the atmosphere of Venus (e.g., see Marov and Ryabov[11]).

The value of the integral G [Eq. (16)] obtained from numerical integration of the pressure distribution behind a strong shock wave (Sedov[12] and Korobeinikov et al.[13]) was found to be $G = 0.22$ and 0.23 for $\gamma = 1.4$ and 1.3, respectively.

Calculated values of f_1 and f_2 are given in Table 3. For an ambient gas with a smaller value of $\gamma (= 1.3)$ than 1.4, the specific impulse would be reduced by about 6% via the function f_1, and for conditions for which the integral H is negative and rarefaction effects become important, the larger value of f_2 (10% higher) would also lead to reduced performance.

Table 3 Values of functions f_1 and f_2 for $\gamma = 1.3$ and 1.4

γ	α	G	f_1	f_2
1.3	1.15	0.23	0.093	9.40
1.4	0.851	0.22	0.099	8.50

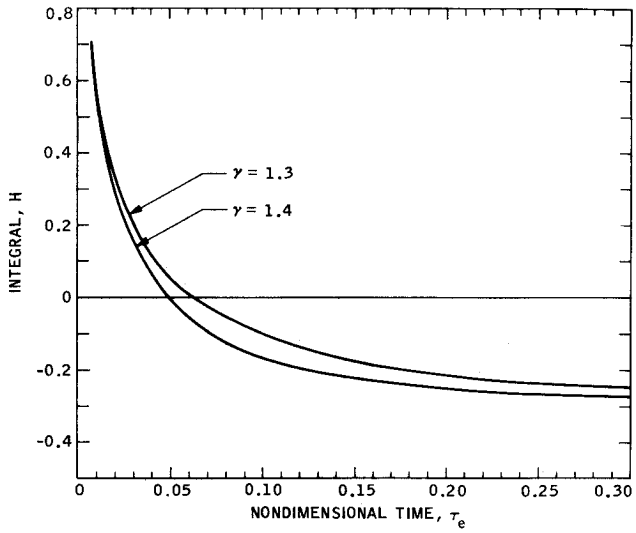

Fig. 4 Variation of integral H with τ_e for $\gamma = 1.3$ and 1.4.

The integral $H(\tau_e)$ is also dependent on γ through the variation of the plateau pressure ratio P_o/P_a with time as well as the nondimensional time τ_e when the shock wave reaches the nozzle exit. From Ref. 5 the relationship between τ_e and r_e/R_l is given as follows in the strong shock limit

$$\tau_e = (\alpha\gamma/4\pi)^{1/2}(r_e/R_l)^{5/2} \tag{18}$$

where for $\gamma = 1.4$ and 1.3, values of $[(\alpha\gamma/4\pi)]^{1/2}$ are 0.309 and 0.345, respectively.

Values of the plateau pressure ratio P_o/P_a for the case of a finite back pressure or counterpressure were obtained from Korobeinikov et al.[14] for $\gamma = 1.3$, and the value of the integral $H(\tau_e)$ [Eq. (16)] obtained by numerical integration is given in Fig. 4 along with the value for $\gamma = 1.4$ obtained in Ref. 5. Larger values of τ_e (about 10% higher for $\gamma = 1.3$) increase the value of H for a given value of r_e/R_l and therefore tend to increase the performance.

In general, the influence of detonating explosives in an ambient, triatomic gas like carbon dioxide is difficult to ascertain a priori with regard to the γ effect because of the competing trends. The specific impulse [Eq. (14)] also depends upon ambient gas density ρ_a and pressure P_a. The dependence on pressure is contained in the expression for the characteristic length R_l, Eq. (17). Note that τ_e depends upon R_l, and thus $H(\tau_e)$ also depends upon R_l. The rather complicated dependence of the specific impulse on ambient gas and conditions indicated from conical flow theory is seen subsequently.

Comparison Between Ideal Conical Flow Theory and Experiments

Since the various length nozzles had a flat endwall, the theory was adapted to the actual nozzles by adding a conical section of length a to the nozzles so that the effective radial length was r_e (see Fig. 5).

Predictions from conical flow theory [Eq. (14)] are shown in Fig. 3. These predictions are shown for the nitrogen data for values of σ as low as unity, although the theory is not expected

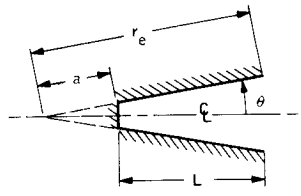

Fig. 5 Results from conical flow model and experimental data for larger σ (see Table 4).

Table 4 Results from conical flow model and experimental data for larger σ,[a] $\theta = 10°$

Ambient gas	L, cm Actual nozzle	r_e, cm	V, cm^3 Actual nozzle	P_a, bars	σ	r_e/R_l	τ_e	H	f_3	I, sec Predicted	I, sec Exp.
Nitrogen	15.2	21.9	320	6.9	1.62	0.45	0.042	+0.056	+0.085	207	
at T_a =				8.3	1.95						270
298°K				13.8	3.24	0.57	0.075	−0.11	−0.19	219	
				27.6	6.48	0.72	0.13	−0.20	−0.39	233	
				41.4	9.72	0.82	0.19	−0.24	−0.49	240	
				57.9	13.6	0.92	0.25	−0.26	−0.56	243	
				69.0	16.2	0.97	0.29	−0.27	−0.60	244	290
	11.4	18.0	174	8.3	1.06						250
				13.8	1.77	0.47	0.046	+0.024	+0.037	209	
				27.6	3.53	0.59	0.082	−0.13	−0.22	221	
				41.4	5.30	0.67	0.11	−0.19	−0.34	230	
				57.9	7.42	0.75	0.15	−0.22	−0.43	236	
				69.0	8.87	0.80	0.18	−0.23	−0.47	239	279
	7.6	14.1	80	8.3	0.49						254
				27.6	1.63	0.46	0.045	+0.033	+0.051	208	
				41.4	2.44	0.53	0.063	−0.069	−0.11	215	
				57.9	3.41	0.59	0.083	−0.13	−0.23	222	
				69.0	4.1	0.63	0.096	−0.16	−0.28	225	267
Carbon	15.2	21.9	320	1.0	0.37						255
dioxide				25.3	9.5	0.70	0.14	−0.16	−0.34	288	307
at T_a =				47.3	20.7	0.86	0.23	−0.23	−0.52	308	338
308°K				69.7	42.0	0.97	0.32	−0.25	−0.61	352	378
				84.5	119.0	1.04	0.38	−0.25	−0.63	563	579

[a] See also Fig. 5 for nomenclature.

to apply at such values since the mass of gas produced by the explosion is not taken into account. The prediction for the small-angle nozzles are about 15% below the nitrogen data and, in terms of the parameter σ, overlap one another like the experimental results. A prediction was made for the large half-angle nozzle too, although the one-dimensional theory is not expected to be applicable.

There is also relatively good agreement with the carbon dioxide data obtained with the small-angle nozzle. In the prediction, the ideal triatomic gas value of $\gamma = 1.3$ was used and the result from Eq. (14) based on perfect gas behavior was applied directly even in the vicinity of the critical point where the perfect gas relation ceases to apply.

The agreement between conical flow theory and both the nitrogen and/or air data and the carbon dioxide data is perhaps better than expected based on the assumptions that were made in the analysis and the application. The analysis is discussed further in Ref. 5 with regard to the refilling phase which is treated in an idealized way in the present calculations.

One reason for the better agreement between the conical flow predictions and the experiments is believed to be associated with the weaker dependence of specific impulse on ambient gas density (or σ) than indicated from the global considerations. In this regard, values of the second term in brackets in Eq. (14), denoting it as

$$f_3 = \frac{15}{32(\pi)^{1/2}} f_2 H \left(\frac{r_e}{R_l}\right)^{1/2} \tag{19}$$

are shown in Table 4. They become negative because of rarefaction effects as σ increases, and therefore the term $1+f_3$, and thus the specific impulse is reduced. For the carbon dioxide data the effect of rarefaction may have reached a limiting condition so that the prediction tends toward the same slope as the global considerations for ideal performance (Fig. 3).

The gross behavior implied in the conical flow model is that as the ambient density or pressure increases, the characteristic length R_l decreases, and consequently the strength of the shock wave and thus flow speeds behind the shock wave become less. The velocity of the ambient gas exhausted from the nozzle consequently is reduced relatively more than that obtained from global considerations for complete conversion of thermal to kinetic energy

$$\bar{u} = (2g_c)^{1/2}(e_a)^{1/2}[1/(1+\sigma)^{1/2}] \tag{20}$$

VI. Venus Probe Calculations

Calculations were carried out for atmospheric conditions on Venus from the surface to an elevation of 35 km. The pressure, temperature, and density at 5 km intervals given by Marov and Ryabov[11] are tabulated in Table 5. For this range of conditions,

Table 5 Venus calculations

Z, km	T_a, °K	P_a, bars	ρ_a, gm/cm^3	σ	r_e/R_l	τ_e	H	I, sec
0	750	95.2	6.57×10^{-2}	14.0	1.08	0.42	−0.25	186
5	710	69.6	5.11	10.8	0.97	0.32	−0.25	179
10	670	49.9	3.90	8.21	0.87	0.24	−0.23	188
15	629	35.1	2.93	6.15	0.77	0.18	−0.20	197
20	587	24.0	2.15	4.50	0.68	0.13	−0.15	204
25	545	16.0	1.55	3.23	0.60	0.095	−0.088	210
30	502	10.3	1.09	2.25	0.51	0.066	−0.011	207
35	457	6.4	7.4×10^{-3}	1.55	0.44	0.044	+0.080	198

the primary atmospheric constituent, carbon dioxide, can be considered to be a perfect gas with $\gamma = 1.3$. The calculations were carried out for 1.5 g data sheet, the same explosive as used in the experiments, and for the 10°, 15.2 cm nozzle ($r_e = 21.9$ cm).

The results of the calculations are shown in Table 5 in terms of the specific impulse and the relative mass of ambient gas in the nozzle, σ. Increases in the value of σ correspond to approaching the Venus surface. The specific impulse of about 200 sec is approximately constant as the surface is approached, and this primarily occurs because of the increasing ambient temperature and the importance of rarefaction effects which reduce the specific impulse. The performance however would exceed that for a chemical propulsion system as can be observed by comparison to Fig. 1. The detonation propulsion performance may be improved if rarefaction effects were partially eliminated by allowing the nozzle to refill by drawing in ambient gas through slots in the sidewall (porous nozzle).

VII. Summary

Detonation propulsion experiments have been carried out with nitrogen and air, and carbon dioxide as the ambient gas to reveal the magnitude of the specific impulse and its increase with the relative mass of ambient gas in the nozzle. The measurements indicated that the performance would exceed that of a monopropellant. The experimental trends are in general agreement with global considerations, and specific application of ideal blast wave theory yielded estimated specific impulses that compared favorably with the measurements.

Appendix

Chemical Propulsion

To provide a reference basis for appraising the performance of a detonation propulsion system, the following relation for the specific impulse was evaluated for steady isentropic flow in a chemical propulsion system

$$I = \lambda u_e/g_c + (P_e - P_a)A_e/\dot{m} \tag{21}$$

where the exit velocity is given by

$$u_e = \{2\gamma RT_t(\gamma-1)^{-1}[1-(P_e/P_t)^{(\gamma-1/\gamma)}]\}^{1/2} \tag{22}$$

and the mass flow rate for choked flow is

$$\dot{m} = C_D P_t A_{th}\left[\frac{\gamma}{RT_t}\left(\frac{2}{\gamma+1}\right)^{(\gamma+1)/(\gamma-1)}\right]^{1/2} = \frac{C_D f(\gamma) P_t A_{th}}{(RT_t)^{1/2}} \tag{23}$$

Introducing Δp as the difference between the stagnation pressure P_t in the nozzle and the ambient pressure P_a, i.e.,

$$\Delta p = P_t - P_a \tag{24}$$

then the specific impulse can be written as follows to indicate the explicit dependence on the parameters involved

$$I = \lambda u_e/g_c + [P_e/P_t - P_a/(\Delta p + P_a)](RT_t)^{1/2}[C_D f(\gamma)]^{-1}\varepsilon \tag{25}$$

For a given gas at a stagnation temperature T_t and a flow coefficient C_D and divergence factor λ, the specific impulse depends upon the expansion area ratio ε of the nozzle and the ambient pressure for a specified value of Δp since both the exit velocity and exit pressure ratio P_e/P_t depend only upon ε.

Values obtained from Eq. (25) are discussed in the introduction and shown in Fig. 1. The calculations were terminated at an ambient pressure $P_{a_{\max}}$ so that shock-induced flow separation would not occur in the nozzle by using the Summerfield criterion

$$P_e \simeq 0.4\, P_{a_{\max}} \tag{26}$$

From Eqs. (24) and (26) and the functional relationship $P_e/P_t(\gamma, \varepsilon)$, the following dependence of $P_{a_{\max}}$ on Δp and ε is obtained

$$P_{a_{\max}} = \Delta p \Big/ \left[\frac{0.4}{(P_e/P_t)} - 1\right] \tag{27}$$

For the sonic nozzle $\varepsilon = 1$, calculations were also made for unchoked flow by using the appropriate mass flow rate. These values are also shown in Fig. 1.

References

[1] Beichel, R. and O'Brien, C. J., "Explosive Propulsion Status Report," ALRC Rept. ASG-7001, March 1970, Aerojet General Corp., Sacramento, Calif.

[2] Gross, M., "Explosive Impulse Calculations," PIFR 259, Nov. 1970, Physics International Co., San Leandro, Calif.

[3] Bestgen, R. F. and Nunn, J. R., "Propulsion Performance of Condensed-Explosive Rockets," AIAA Paper 72-1161, New Orleans, La., 1972.

[4] Varsi, G., Back, L. H., and Dowler, W. L., "Development of Propulsion for High-Atmospheric-Pressure or Dense Environments," *Jet Propulsion Lab. Quarterly Tech. Rept.*, Vol. 3, No. 2, July 1973, pp. 45–52.

[5] Back, L. H., "Application of Blast Wave Theory to Detonation Propulsion" (to be published).

[6] Varsi, G., "Detonation Propulsion," *Chemical Propulsion Agency Newsletter*, April 1973, p. 1.

[7] Michels, A., Blaisse, B., and Michels, C., "The Isotherms of CO_2 in the Neighborhood of the Critical Point and Round the Coexistence Line," *Proceedings of the Royal Society (London)*, Ser. A., Vol. 160, 1937, pp. 358–375.

[8] Michels, A. and Michels, C., "Isotherms of CO_2 Between 0° and 150° (C) and Pressures from 16 to 250 atm," *Proceedings of the Royal Society (London)*, Ser. A, Vol. 153, 1935, pp. 201–214.

[9] Gill, S., private communication, Jan. 1973, Artec Associates, Hayward, Calif.

[10] Menichelli, V. J., "Sensitivity Data Obtained on a Variety of Explosive Mixtures Intended for Laser Initiation," private communication, July 19, 1973, Jet Propulsion Lab., Pasadena, Calif.

[11] Marov, M. Ya. and Ryabov, O. L., "Model of Venus Atmosphere," Rept. to Working Group VII of COSPAR, 1972.

[12] Sedov, L. I., *Similarity and Dimensional Methods in Mechanics*, Academic Press, New York, 1959, p. 222.

[13] Korobeinikov, V. P., Chushkin, P. I., and Sharovatova, K. V., "Tables of Accurate Gas Dynamic Functions of the Initial Phase of Explosions," Issue 2, 1963, Computing Center of Academy of Sciences, USSR, Moscow (in Russian).

[14] Korobeinikov, V. P., Chushkin, P. I., and Sharovatova, K. V., *Accurate Gas Dynamic Function for Explosions*, edited by V. P. Karlikov, Computing Center of Academy of Sciences USSR, Moscow, 1969 (in Russian).

[15] *The Planet Jupiter (1970)*, NASA SP-8069, 1971.

[16] *The Planet Saturn (1970)*, NASA SP-8091, 1972.